Applied Geography 112 (2019) 102096

Contents lists available at ScienceDirect

Applied Geography

journal homepage: http://www.elsevier.com/locate/apgeog

Quantitative assessment of urbanization and impacts in the complex of Huế Monuments, Vietnam

Van-Manh Pham [a,b,*], Son Van Nghiem [c], Quang-Thanh Bui [a,b], Tam Minh Pham [b], Cu Van Pham [b]

[a] Center for Applied Research in Remote Sensing and GIS (CARGIS), 334 Nguyen Trai, Thanh Xuan, Ha Noi, Viet Nam
[b] Faculty of Geography, VNU University of Science, 334 Nguyen Trai, Thanh Xuan, Ha Noi, Viet Nam
[c] NASA Jet Propulsion Laboratory, California Institute of Technology, 4800 Oak Grove Drive, MS 300-235, Pasadena, CA, 91109, USA

ARTICLE INFO

Keywords:
Complex of Huế Monuments
Ecosystem services
Environmental impact
Historical monuments
Land cover and land use
Object classification
Remote sensing
Support vector machine
Urbanization
Vietnam

ABSTRACT

Rapid and extensive urban changes in recent decades have inflicted a multitude of challenges in land-use planning and conservation management, especially for the heritage protection of historic areas. This paper describes the results of an integrated approach to analyzing the potential environmental impacts of urbanization that has profoundly transformed land cover and land -use in Vietnam. A combination of remote-sensing techniques and ancillary indices enables a quantitative evaluation of urbanization impacts on 12 sites in the Complex of Huế Monuments, a UNESCO World Heritage Site, from 1968 to 2016. This approach includes classifying satellite images, analyzing urbanization characteristics with land-cover and land-use change and urbanization indices, and quantifying environmental impacts by ecosystem service values. Object-based classification results indicate that the support vector machine algorithm achieves an optimum overall accuracy of 84.78–86.5% and a Kappa coefficient of 0.82–0.84. Quantitative results of the total absolute loss value reveal the largest negative effect at Huế Citadel and the most positive at Tự Đức Tomb, with the overall consequence of urbanization being predominantly negative for the whole complex. The adverse impacts are found primarily from the degradation of agriculture and green space. The negative total loss value also serves as a quantification of impacts from increased urbanization on human well-being. This integrated methodology can be a potentially effective tool to plan for sustainable development in the continual trend toward further urbanization in Vietnam.

1. Introduction

In land-use science, urbanization is defined as the combination of many processes, including population growth, immigration, and the demand for living space, landscape types and necessary infrastructures, conducing to profound impacts on developing countries (Schneider et al., 2012; UN-Habitat, 2013; Zhang & Su, 2016). These processes may lead to urban heat-island effects, air and water pollution, aggravated disasters, and excessive demand for energy use and waste treatment (Guo, Zhang, & Li, 2010; He, Liu, Tian, & Ma, 2014; Zhou, Qian, Li, Li, & Han, 2014). These negative impacts of urbanization can accelerate the transformation of land-use types, which forces conflicting decisions in urban development planning (Liu, He, Zhang, Huang, & Yang, 2012; Maes et al., 2015; Marull, Font, & Boix, 2015). Scattered and irregular patterns of land cover and land use (LCLU) make landscapes haphazardly heterogeneous in space and in time, hindering LCLU sustainability by a disarray of changes in the environment. In this respect, monitoring urbanization is critical to timely identifying challenges to be addressed by researchers, planners, and decision-makers (Kane, Connors, & Galletti, 2014; Liu & Yang, 2015; Su, Ma, & Xiao, 2014).

The analysis of ecological services (ES) has emerged as a way to link natural factors with cultural resources for developing sustainable land use (Hølleland, Skrede, & Holmgaard, 2017; Millennium Ecosystem Assessment, 2005). Particularly, in terms of the cultural heritage, the integration of ES in the conservation management at the heritage sites could effectively addressed issues of cultural diversity, knowledge systems, educational values, and social relations (Gearey, Fletcher, & Fyfe, 2014; Hølleland et al., 2017; Tengberg et al., 2012). The increase or decrease in ecosystem values helps determine the potential capacity of various benefits or disservices of the impacts in the context of urbanization (Haas, 2016; Haas & Ban, 2014). Because these linkages are dynamical, monitoring the ES is imperative to assess LCLU as social

* Corresponding author. Center for Applied Research in Remote sensing and GIS (CARGIS), 334 Nguyen Trai, Thanh Xuan, Ha Noi, Viet Nam.
E-mail address: manh10101984@gmail.com (V.-M. Pham).

https://doi.org/10.1016/j.apgeog.2019.102096
Received 17 October 2018; Received in revised form 8 August 2019; Accepted 8 October 2019
Available online 17 October 2019

resources (Mörtberg et al., 2013).

Long-term continuity of satellite observations of land cover is key to determining their variability, assessing changes, and managing ecosystems. The increasing number of recent remote-sensing studies to quantify ecosystem services gives rise to potential methods to determine and evaluate landscape functions (Feng, Fu, Yang, & Lü, 2010; Lakes & Kim, 2012). Primarily, these values can serve as indicators of ecological conditions and functions (Bolund & Hunhammar, 1999; Costanza, d'Arge, & de Groot, 1997), which have attracted extensive conceptual research in urban spaces through various valuation schemes and remote-sensing tools (Feng et al., 2010; Palacios-Orueta et al., 2012; Ustin et al., 2004; Xie, Zhen, Lu, Xiao, & Chen, 2008). Additionally, relationships among green space, infrastructures, and urbanization can be examined to quantify environmental impacts in a region (Maes et al., 2015; Verbeek, Boussauw, & Pisman, 2014).

Many studies use remotely sensed data as the primary resources to extract information about urbanization processes (Chen, Liu, & Lu, 2016; Kuang, Chi, Lu, & Dou, 2014; Li, Li, & Wu, 2013; Song, Sexton, Huang, Channan, & Townshend, 2016; Zhao et al., 2015). Nevertheless, past studies suffered significant limitations from satellite images with a medium and low spatial resolution (Huang, Schneider, & Friedl, 2016; Small & Elvidge, 2013; Yi, Zeng, & Wu, 2016; Zhang & Seto, 2011; Zhao et al., 2015). In contrast, detailed information derived from high-resolution data is required for observations of heterogeneous urban areas (Bhaskaran, Paramananda, & Ramnarayan, 2010; Deng, Wang, Hong, & Qi, 2009; Dewan & Yamaguchi, 2009; Gao, Huang, He, Sun, & Zhang, 2016; Liu et al., 2012) with complex data collections to obtain reliable information of LCLU changes (Ban, Jacob, & Gamba, 2015; Ban & Jacob, 2013; Niu & Ban, 2013). Thereby, the concept of ecological services can be applied to evaluate environmental impacts (Furberg, 2014; Tianhong, Wenkai, & Zhenghan, 2010), and to determine influences of urbanization on the natural environment in terms of numerous indicators (Aldwaik & Pontius, 2012; Estoque & Murayama, 2015; Kantakumar, Kumar, & Schneider, 2016). Despite some limitations in consistency and quantity of satellite data (Syrbe & Walz, 2012), the number of these studies has been increasing (Alamgir, Pert, & Turton, 2014; Lakes & Kim, 2012). For each location, these methods need to be customized effectively to account for specific local conditions (De Groot et al., 2012). Few researchers have addressed urbanization impacts by integrating ecological services with various spatial attributes.

In this paper, we present an analysis of LCLU changes for the Complex of Huế Monuments, consisting of 12 heritage sites, using multitemporal remote-sensing data to assess environmental impacts due to urbanization. The main objectives of this study include quantifying urbanization characteristics in the period of 1968–2016 using object-based Support Vector Machine (SVM) classification, calculating the urbanization indices representing growth rates of LCLU transformations, and measuring values of ecological services with relations between human impacts and environment.

2. Study area and method

2.1. Description of the study area

In Vietnam, the Complex of Huế Monuments epitomizes rich historical architectural and cultural achievements, demonstrating the last Vietnamese feudal power at its peak in the early 19th century (ICOMOS, 1992). The structure of this site follows the astrological alignment. Specifically, it represents the five cardinal points (east, west, north, south, and center) corresponding to the five natural elements (earth, metal, wood, fire, and water) (HMCC, 2015). The historical and cultural values remain evident in the remnants of the monuments even after significant impacts from three major military conflicts in 1885, 1947, and 1968 (ICOMO, 1992). To study effects of recent urbanization since the year of the last major military impact, 1968 was selected as the beginning of the period of investigation for this study.

These monuments have suffered from the development of human settlement in the vicinity. Although the complex has been inscribed in the list of the United Nations Educational, Scientific, and Cultural Organization (UNESCO) World Heritage Sites since 1993, efforts to preserve the monuments' integrity have faced many challenges inflicted by socioeconomic development priorities (HMCC, 2015). For this reason, maintaining the essential cultural features as well as the surrounding natural landscape and ecological conditions has become a fundamental problem (HMCC, 2015; ICOMOS, 1992).

The study area encompasses the Complex of Huế Monuments, consisting of: Huế Citadel (H1), Thiên Mụ Pagoda (H2), Temple of Letters and Temple of Military (H3), Royal Arena and Voi Ré Temple (H4), Dục Đức Tomb (H5), Nam Giao Esplanade (H6), Tự Đức Tomb (H7), Hòn Chén Temple (H8), Thiệu Trị Tomb (H9), Khải Định Tomb (H10), Minh Mạng Tomb (H11), and Gia Long Tomb (H12) (). The process of rural-to-urban transformation has introduced additional urban features into the landscape in this area. In monitoring this dynamical transformation, relevant information was extracted from multitemporal remote-sensing data and geographic information system (GIS) methods (Zhang & Su, 2016). In this study, remote-sensing and ancillary data in the nearly semi-centennial period of 1968–2016 were used to distinguish multiple LCLU classes, including high-density built-up areas (HDB), low-density built-up areas (LDB), agriculture (AGR), water bodies such as lakes and rivers (WT), forest (FR), greenery (UGS), bare soil (BS), and cemetery (CEM).

2.2. Methodology

2.2.1. Image preprocessing and object-based classification

2.2.1.1. Satellite image preprocessing and ancillary data. To determine the trend of urbanization in the study area, the main spatial data used in this study consisted of detailed survey maps for the year of 1968 from the National Imagery and Mapping Agency (NIMA), digital elevation model (2.5-m) together with aerial photographs, and high-resolution satellite images in 1995 (Satellites Pour l'Observation de la Terre SPOT 3 - March 17 with 10-m panchromatic and 20-m multispectral resolution capability) and in 2016 (SPOT 7 - September 20 with 1.5-m panchromatic and 6-m multispectral resolution capability) (Table 1). All SPOT images are cloud-free and acquired between March and September of each respective year. These multitemporal satellite images are calibrated, and radiation/atmospheric effects are removed by using the COSine Theta (COST) method. With the surface reflectance taken to be to 1% of dark objects in the images, the value of radiance difference is obtained by subtracting the values from different images corresponding to each image pixel (Chavez, 1996). These images are projected to the WGS84 coordinate system/UTM zone 48N with ground-control points and orthorectified by using digital elevation model data, which ensure the geometric correction accuracy of about ±0.5 pixel. The data are further improved by image enhancement techniques to account for phenological and seasonal effects occurred at different times to detect LCLU changes. Image processing steps are implemented to regrid data into the same resolution of 2.5-m in order to prepare for the extraction of LCLU information with high accuracy in each 500-m^2 square mask.

Survey maps in 1968, available for this overall study area at a scale of 1:50,000 and for the Huế Citadel area at a scale of 1:12,500 (Table 1), were downloaded from NIMA as published by the University of Texas Libraries (NIMA, 1968a; 1968b). These data were digitized, edited, and used to derive the LCLU information together with additional ancillary GIS data from the Department of Survey, Mapping and Geographic Information of Vietnam (2017). These maps contain a wealth of necessary information, including topography and other land-surface details relevant to the various LCLU classes. Primarily, high-density built-up areas (HDB) was used in this study for areas of prominent and non-prominent buildings, low-density built-up areas (LDB) for built-up areas,

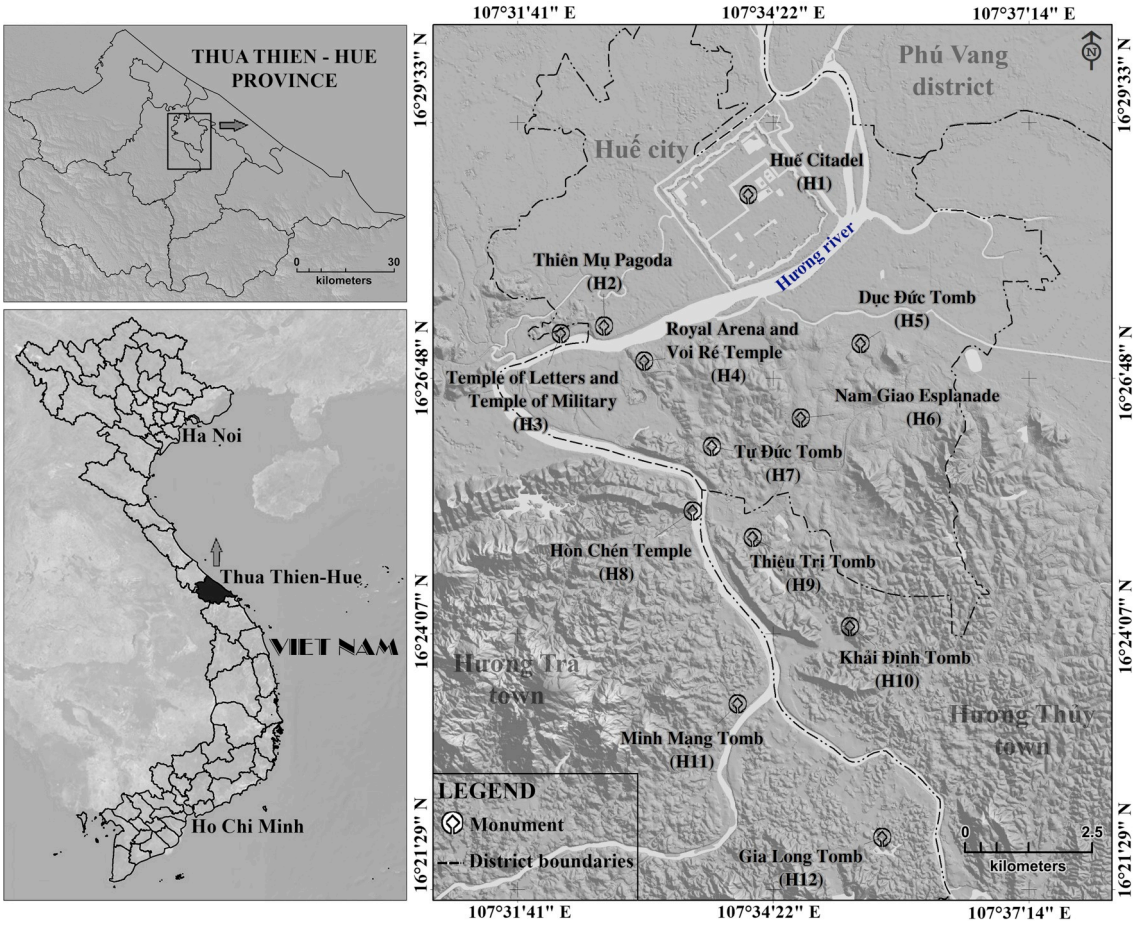

Fig. 1. Overall map of the study area in Phú Vang district of the Thừa Thiên-Huế province (left panel), and locations of 12 historical sites in the Complex of Huế Monuments (right panel).

Fig. 2. Photographs taken on 24 December 2015: Ngọ Môn Entrance of the Imperial City in the center of Huế Citadel (left panel) and the tomb of Emperor Tự Đức in the complex of Tự Đức Tomb (right panel). Among the 12 heritage sites in the Huế Complex, Huế Citadel has suffered the largest negative effect from urbanization, and Tự Đức Tomb has experienced the largest positive effect, as shown in this study. For aerial views and photographs of other monuments, see the Management Plan of the Complex of Huế Monuments (HMCC, 2015).

agriculture (AGR) for agricultural rice-field groupings, water bodies (WT) for combinations of water bodies (lake, ponds, rivers, etc.), forest (FR) for plantations and woods/brushwoods, greenery (UGS) for grassland and forested areas, bare soil (BS) for sand classes, and cemetery (CEM) for cemetery areas as noted in the NIMA maps. Specific areas corresponding to the different LCLU classes, staying persistent in the study period, are selected as training samples in the SVM classification of remote-sensing data (see flowchart in Fig. 4).

2.2.1.2. Object-based classification by support vector machine algorithm.

(i) *Segmentation:* In recent years, given the increased spatial resolution of available remote-sensing data, methods of object-based image analysis (OBIA) have become a common preference by researchers over traditional pixel-based methods (Blaschke, 2010; De Pinho, Fonseca, Korting, de Almeida, & Kux, 2012). Basic image-segmentation processing (Fig. 3) is applied to extract object extents with a high accuracy (Shackelford & Davis, 2003) to improve the classification capability, especially for discriminating urban features (Corbane et al., 2015; Myint, Gober, Brazel, Grossman-Clarke, & Weng, 2011; Niu & Ban, 2013). However, no single set of object rules or parameters can determine whether the segmentation results are good or not. Thus, it is also necessary to integrate adjacent pixels with similar spectral characteristics, the mean size of objects, and their homogeneity (Pu, Landry, & Yu, 2011). Each segmented patch in a given image is assigned to only

Fig. 3. A sample of image segmentation at Scale of 10, Shape of 0.75, and Compactness of 0.5 for a SPOT satellite image acquired in 2016 at the Minh Mạng Tomb (H11).

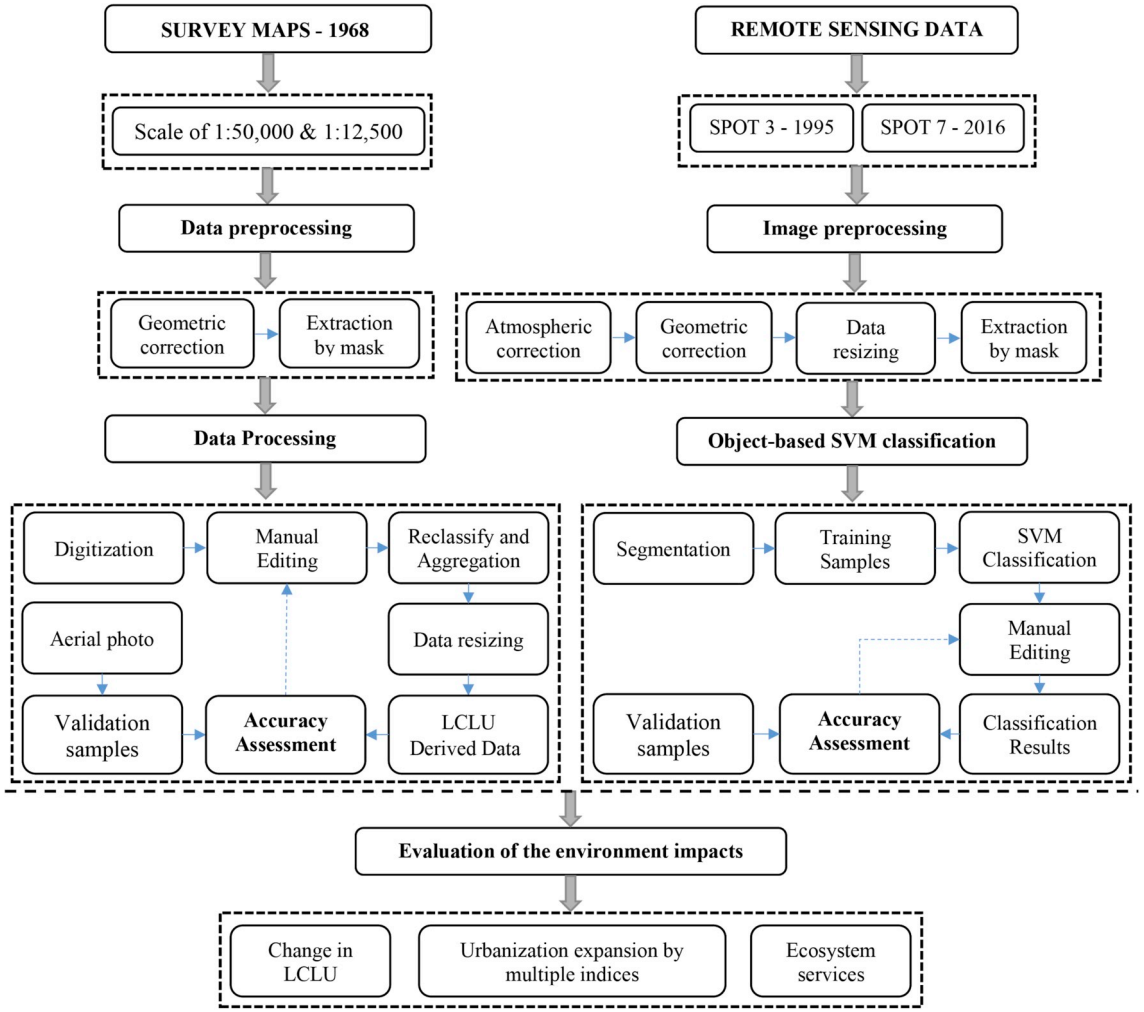

Fig. 4. Flowchart of the methodological framework used in this study.

one corresponding class associated with the object data (Zhou, Huang, Troy, & Cadenasso, 2009). Therefore, the fitting-value selection of the shape, scale, and compactnessparameters will collectively determine object accuracy for the LCLU classification step.

(ii) Image classification by SVM algorithm: The many algorithms integrated into OBIA classification include Bayes, Decision Tree, and k-Nearest Neighbor to make different machine-learning classifiers. These methodologies have been proven very effective for feature extraction from high-resolution images (Gao, Tang, Jing, Li, & Ding, 2017). Based on performance comparisons in many research studies, the SVM algorithm has been found more efficient than other methods (Malinverni et al., 2011; Qian, Zhou, Yan, Li, & Han, 2014; Zhang, Feng, & Jiang, 2010). In the SVM classification of two classes given n points in d-dimensional space (each point belonging to a class notation of $+1$ or -1), the purpose is to find a hyperplane partition optimized for the separation of these points into two parts so that the same type of LCLU stays within each partition with the sample data set separated by $\{(x_1,y_1), (x_2,y_2), \ldots, (x_n,y_n)\}$ where $x_i \in R^d$ and $y_i \in \{\pm 1\}$. The optimal hyperplane assigns this dataset into two categories of LCLU with the largest margins (Cortes & Vapnik, 1995). In the case of no anterior information available for the underlying data distribution, the SVM algorithm allows self-adaptability, a quick learning step, and limited necessities on training sample size (Duro, Franklin, & Dubé, 2012). In this study, the SVM algorithm in object-based classification was implemented with PCI Geomatics 2017 software, Service Pack 4 (trial version).

(iii) Accuracy assessment and manual editing: During the classification process, the results were further calibrated by a manual editing step. An additional accuracy assessment was performed on the final classification after the combination of subclasses but before post-classification refinements. These steps were applied on a set of 600 samples for the 12 sites (H1 to H12) in the Complex of Huế Monuments were selected by the stratified random sampling method with 420 samples (70%) for training and 180 samples (30%) for validation. For each map, a confusion matrix was created from the comparison of the differences between the classification results and corresponding validation points. The overall accuracy was determined through the Kappa coefficient, presented in detail in published literature (Erener, 2013; Pontius & Millones, 2011).

2.2.2. Urbanization indices and ecosystem services

2.2.2.1. Urbanization indices (UIs). As a simple indicative measurement of urban growth, urbanization indices have been developed to quantify the landscape change from multiple satellite images (Bolund & Hunhammar, 1999; Liu et al., 2012). These indices describe the characteristics of dynamic patterns in space. The present study utilized four formulas for Annual Increase (AI), Annual Expansion Rate (AER), Urban Land Percentage (ULP), and Urban Green Infrastructure (UGI). The AI (Equation (1)) indicator describes the relative measurement of the rate (%) of urban change through the comparison of urban areas at two different times. The AER (Equation (2)) indicator presents the overall rate (%) of change of urban areas throughout the entire period of 48 years with $t_1 = 1968$ and $t_2 = 2016$. The ULP (Equation (3)) indicator is defined as the ratio between an urban area and total area at a specified point in time. Moreover, the UGI (Equation (4)) indicator is a quantification of UGS change in comparison with simultaneous urban growth. These indicators provide the relevant quantitative information to characterize the change in urban areas, which are determined by the following equations:

$$AI = \frac{Area_{(t2)} - Area_{(t1)}}{Area_{(t1)}} \times 100\% \quad \text{(Equation 1)}$$

$$AER = \left[\left(\frac{Area_{(t2)}}{Area_{(t1)}} \right)^{1/48} - 1 \right] \times 100\% \quad \text{(Equation 2)}$$

$$ULP = \frac{Area_{(t2)}}{Area_{(total)}} \times 100\% \quad \text{(Equation 3)}$$

$$UGI = \frac{UGS_{(t2)} - UGS_{(t1)}}{\left(HDB_{(t2)} + LDB_{(t2)}\right) - \left(HDB_{(t1)} + LDB_{(t1)}\right)} \times 100\% \quad \text{(Equation 4)}$$

where $Area_{(t2)}$ is the total urban land in the year after; $Area_{(t1)}$ is the total urban land in the year before; $Area_{(total)}$ is the total land surface; HDB is the amount of high-density built-up land; and LDB is the amount of low-density built-up land.

2.2.2.2. Ecosystem services (ES). Ecosystem services are defined as human benefits gained from impacts to the environmental system due to changes in the urban area with heterogeneous patterns. The measurement of ecosystem services is derived from the degree of ecosystem functions used to serve humans (Costanza et al., 1997). The value of ecosystem services is the price in monetary units (MU) of environmental factors in maintaining sustainable human well-being (Luisetti, Jackson, & Turner, 2013). In fact, even though these values do not fully describe the drivers in the ecosystem, the relative differences or similarities among them can quantify the degree of change of the human-environment relationship. Based on comparisons of their results, different urbanization trends reflect emerging challenges for humans of LCLU change. In this study, Table 2 describes the LCLU classes and quantifies corresponding biomes and ecosystem services values per hectare, the valuation of ecosystem services consisted of estimating the approximate monetary values in monetary unit (MU) using the updated valuation scheme proposed by (Costanza et al., 2014). According to this scheme, the total biome area is first summed up and then multiplied by a monetary factor, as presented in Eq. (5) given by

$$E = \sum_i (CA_i \times UV) \quad \text{(Equation 5)}$$

where E is estimated ecosystem service value; CA_i is area in hectare of

Table 1
Sensor system characteristics of multi-temporal data series used in this study.

Acquisition date	Type of data used	Spectral mode	Spectral resolution	Spatial resolution/ Scale
2016/09/20	SPOT-7	PAN	0.45 – 0.74 (μm)	1.5-m
2016/09/20	SPOT-7	XS	0.45 – 0.52 (μm): Blue 0.53 – 0.59 (μm): Green 0.62 – 0.69 (μm): Red 0.76 – 0.89 (μm): Near-Infrared	6-m
1995/03/17	SPOT-3	PAN	0.51 – 0.73 (μm)	10-m
1995/03/17	SPOT-3	XS	0.50 – 0.59 (μm): Green 0.61 – 0.68 (μm): Red 0.79 – 0.89 (μm): Near-Infrared	20-m
1968	Survey maps	N/A	N/A	1:12,500
1968	Survey maps	N/A	N/A	1:50,000

PAN: Panchromatic mode; XS: Multispectral mode.

Table 2
Ecosystem services values calculated for the corresponding land cover and land use classes (MU in $/hectare/year, referenced to the 2007 price level).

LCLU	The description of biome	Unit values ($/hectare/year)
HDB	Urban	6,661
LDB	Urban	6,661
AGR	Cropland	5,567
FR	Forest Tropical	5,382
WT	Lakes/Rivers	12,512
UGS	(Forest + Grasslands)/2	7,465

LCLU category *i*; *UV* is ecosystem service unit value expressed in MU/hectare/year.

Ecosystem services are calculated for the main classes namely: High-density built-up (HDB), low-density built-up (LDB), agriculture (AGR), water bodies such as lakes and rivers (WT), forest (FR), greenery (UGS), bare soil (BS), and cemetery (CEM). For UGS, its value is defined by averaging the values of forest and grasslands, whereas the classes of CEM and BS are found insignificant in terms of ecosystem services in the area of this study.

2.2.3. Main steps of the methodological framework

Main steps of the methodological framework are summarized with the flowchart in Fig. 4. The data preprocessing of the survey maps in 1968 involves geometric correction and extraction by mask. Then, the data processing step is implemented with these procedures: (i) Converting information into digital format, (ii) manual editing to check and improve the accuracy of objects, (iii) reclassifying and aggregating data into a raster format, (iv) data resizing, and (v) assessing the accuracy of the results.

For the year 1968 when SPOT was not yet launched, we used aerial photographs (Department of Survey, Mapping and Geographic Information of Vietnam, 2017), which did not contain sufficient information for automatic processing. Thus, we manually matched similar objects in the survey maps and in the aerial photographs to geo-rectify the photographs, from which the land cover types of these areas were determined and used as reference samples for the accuracy assessment.

For years 1995 and 2016, SPOT remote-sensing data are available for use in the image preprocessing step, which accounts for atmospheric correction, geometric correction, data resizing, and extraction by the mask. Then, the object-based SVM classification involves segmentation, training samples, SVM classification, manual editing, and accuracy assessments. The segmentation approach is used to extract spatial information of remotely sensed imagery with multiple resolutions. An ensemble of tests was obtained from which the optimal parameters were determined with image segmentation at the scale level of 10, shape value of 0.75, and compactness of 0.5.

From the SVM algorithm, classification images are obtained to display LCLU information in terms of different spatial heterogeneity classes: High-density built-up (HDB), low-density built-up (LDB), agriculture (AGR), water bodies such as lakes and rivers (WB), forest (FR), greenery (UGS), cemetery (CEM), and bare soil (BS).

Finally, the evaluation step characterizes environmental impacts with three procedures accounting for LCLU change, urbanization by multiple indexes, and value estimation of ecosystem services.

3. Results and discussion

3.1. Classification results for the complex of Huế Monuments in the period of 1968–2016

Classification results are presented in Fig. 5 for each of the 12 sites in the Complex of Huế Monuments from 1968 to 2016, with results obtained from National Imagery and Mapping Agency maps for 1968 and derived from SPOT classification images for 1995 and 2016.

The accuracy assessments for all classification results and aggregated class accuracies for each classification are presented in Table 3. The overall accuracy (OA) is 85.63% for the year of 1968, 84.78% for 1995, and 86.5% for 2016. The statistics of the Kappa coefficient are 0.84, 0.82, and 0.84 for 1968, 1995, and 2016, respectively. These verified accuracy results are acceptable to proceed to next steps because the standard of satellite-derived LCLU classification is about or higher than 85% for OA and 0.75 for the Kappa coefficient, as noted in multiple publications (Deng et al., 2009; Melesse, Weng, Thenkabail, & Senay, 2007; Singh et al., 2017).

The accuracy of WT classification for all 12 sites exceeds 95% in the class average while HDB, AGR, FR, CEM, and BS classifications all exceed 85% accuracy in the class average. UGS seems somewhat problematic, and LDB areas are the most difficult to distinguish. A few FR areas are confused with UGS areas in H8, H9, H10, H11, and H12 monuments. This limitation can be overcome by adding a digital elevation model that is very different over FR and UGS areas. The confusion matrix in Table 2 reveals that the most confused class is LDB, with accuracies not exceeding 70%. However, in 2016, the accuracies of LDB areas exceed 70% of the average, possibly because of better spatial resolution and better image quality in remote-sensing data used. Two major components of LDB areas are buildings and surrounding green spaces or surfaces that can be best observed in good images with high resolution. The difficulty is that both features are considered as one overall entity and not separated in sub-segmentation details into HDB (single-pixel without vegetation) and AGR or UGS. Moreover, there is more than one type of LDB area in the 12 sites. Outside Huế City, there are gardens and greenery in the surroundings of H6, H7, and H9 monuments. In the center of Huế City, LDB areas include most villas or low-rise houses surrounded by UGS, which can be mistaken for UGS containing historic buildings or larger buildings with no residential service functions that represent the cultural values. The largest misclassification occurs between UGS and FR or AGR (with vegetation). FR change in the plain and center of Huế City is a process that is not necessarily limited to existing urban boundaries affecting urban, peri-urban, and rural areas. Through the process of land-use change, urban areas and their boundaries are continually redefined.

3.2. Analyzing the urban expansion by UI and LCLU change

Fig. 6 shows the temporal changes of urban land areas over the nearly semi-centennial period of 1968–2016 to illustrate the typical urban expansion in the 12 sites. The plots show that all of these monuments have undergone a linearly increasing trend, indicating that urbanization has been significant continually from 1968 to 2016. The increase in urban areas has occurred predominately due to AGR reduction around these monument sites. A decrease in UGS and forest areas can be observed as well, whereas WT and BS areas have not changed significantly.

Spatial patterns of the three descriptive indicators are shown in Fig. 7. Considerable Annual Increase (AI) is observed in the ruins in the south of Huế City, west of Hương Thủy and east of Hương Trà Districts, where many of the Huế Monuments are located (Fig. 7, left panel), including Khải Định Tomb (251.5%), Minh Mạng Tomb (138.6%), Thiệu Trị Tomb (101%), and Hòn Chén Temple (96.5%). In Huế City center, notable urbanization has also occurred, such as around the Nam Giao Esplanade (117.4%) and Tự Đức Tomb (122.3%). However, the monument areas in the west of Huế City (Thiên Mụ Pagoda, Royal Arena, and Voi Ré Temple) show only moderate change. Similar results are also observed from Annual Expansion Rate (AER) (Fig. 7, center panel). Values of Urban Land Percentage (ULP) indicate that urban land is higher in Nam Giao Esplanade, Khải Định Tomb, Dục Đức Tomb, Minh Mạng Tomb, Tự Đức Tomb, and Thiệu Trị Tomb, in contrast to those at others sites (Fig. 7, right panel) with more geographically heterogeneous characteristics among the 12 sites.

Table 4 presents Urban Green Infrastructure (UGI) (in ha) for seven of the 12 monument sites as well as the differences in UGI for different

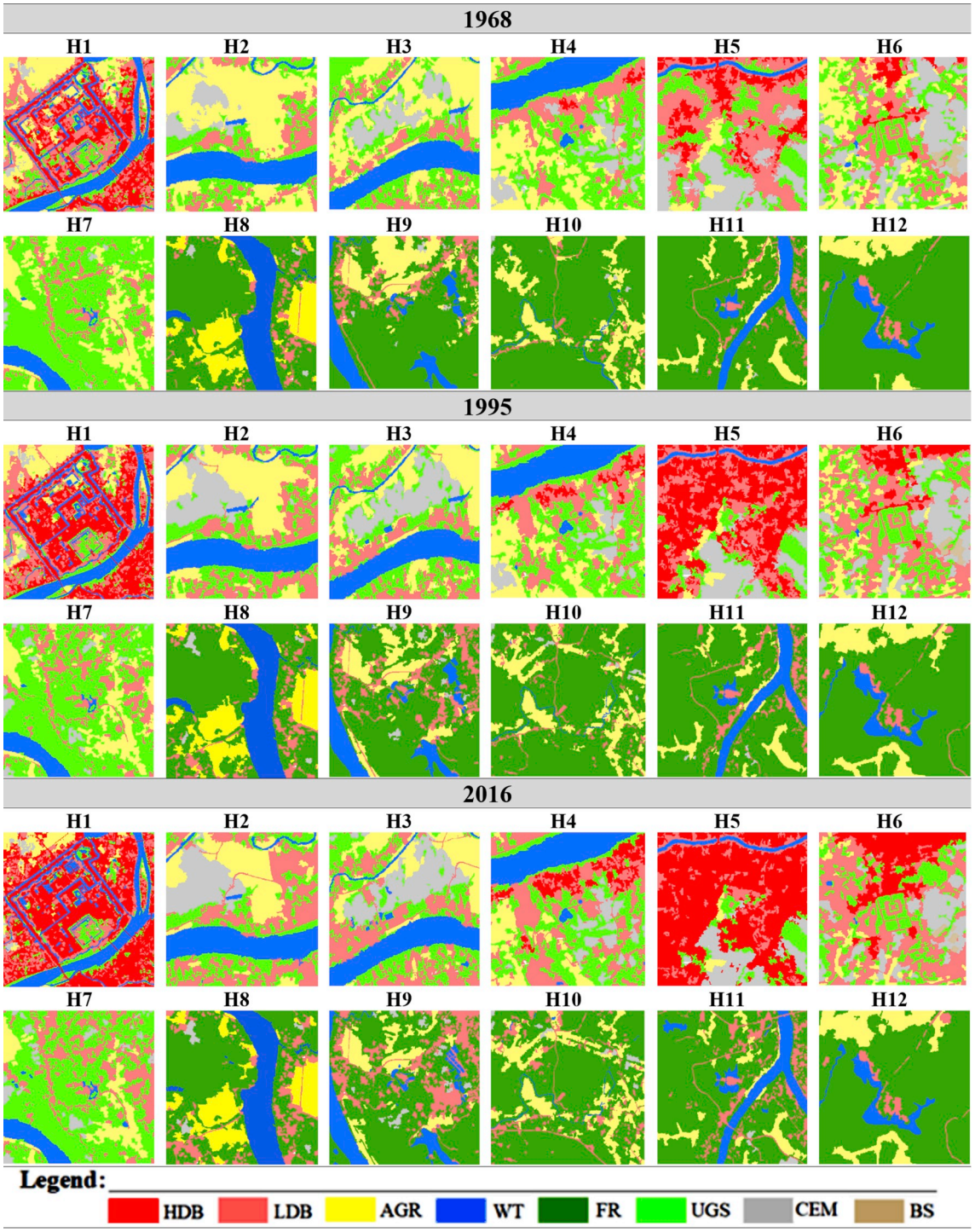

Fig. 5. Classification results of LCLU classes in the period of 1968–2016 for the 12 monument sites: Huế Citadel (H1), Thiên Mụ Pagoda (H2), Temple of Letters and Temple of Military (H3), Royal Arena and Voi Ré Temple (H4), Dục Đức Tomb (H5), Nam Giao Esplanade (H6), Tự Đức Tomb (H7), Hòn Chén Temple (H8), Thiệu Trị Tomb (H9), Khải Định Tomb (H10), Minh Mạng Tomb (H11), and Gia Long Tomb (H12).

years (in %). The UGI index is calculated based on the LCLU classifications from 1968 to 2016. Most monument sites show a detrimental decline in UGS. However, there is a major variability among different sites. For example, Dục Đức Tomb has the largest UGI decrease of 63.2% in nearly five decades, with 23% urban land area. UGI values have also decreased significantly at Huế Citadel (−24.3%) and Tự Đức Tomb (−11.9%) where the urban land area was about 12%. For Nam Giao Esplanade, UGI has reduced by 18.5%, where urban land area accounted for 31% of the total land area.

The above results indicate a continual increase in the urban land observed over each period for all monument sites. Urban land increased by 121% within 27 years (1968–1995) and another 115% in the subsequent 21 years (1995–2016). The total increase in built-up areas was about 236% from 1968 to 2016. The urban expansion rate occurred slightly faster from 1995 to 2016 compared to that from 1968 to 1995. The urban growth in the 12 sites was also apparent but at a slower pace, especially from 1968 to 1995. Meanwhile, urban expansion, occurred more intensely in both speed and spatial extent between 1995 and 2016

Table 3
Aggregated class accuracy, OA and Kappa coefficient for 12 monument sites: Huế Citadel (H1), Thiên Mụ Pagoda (H2), Temple of Letters and Temple of Military (H3), Royal Arena and Voi Ré Temple (H4), Dục Đức Tomb (H5), Nam Giao Esplanade (H6), Tự Đức Tomb (H7), Hòn Chén Temple (H8), Thiệu Trị Tomb (H9), Khải Định Tomb (H10), Minh Mạng Tomb (H11), and Gia Long Tomb (H12).

		H1	H2	H3	H4	H5	H6	H7	H8	H9	H10	H11	H12
1968													
Aggregated class accuracy	HDB	86.5	–	–	88.1	85.5	87.7	–	–	–	–	–	–
	LDB	75.2	70.3	72.1	71.3	69.5	67.3	66.1	64.8	63.7	70.2	71.1	70.5
	AGR	92.1	82.3	84.5	86.2	84.2	87.5	91.1	89.2	89.7	85.6	86.7	87.8
	FR	–	–	–	–	–	–	–	88.8	91.9	87.8	85.5	87.4
	WT	98.8	94.2	95.6	96.7	93.7	97.8	99.5	96.4	97.6	96.9	98.1	97.3
	UGS	80.2	79.3	80.6	82.1	78.7	80.2	78.7	–	–	–	–	–
	CEM	94.5	88.6	87.8	85.9	93.1	89.9	92.2	93.3	90.7	89.9	94.2	–
	BS	–	–	–	–	–	89.9	–	–	–	–	–	–
	OA (%)	87.8	82.8	84.1	85.5	84.1	85.7	85.5	86.5	86.7	86.1	87.1	85.7
	Kappa	0.85	0.81	0.82	0.83	0.82	0.84	0.84	0.85	0.85	0.84	0.85	0.84
1995													
Aggregated class accuracy	HDB	85.4	–	–	87.5	83.8	84.9	–	–	–	–	–	–
	LDB	69.6	70.1	68.3	71.3	69.5	68.2	66.9	65.7	66.5	67	68.1	70.2
	AGR	91.3	82.5	82.5	86.9	85.7	87.9	90.8	87.1	88.8	84.4	85.7	86.8
	FR	–	–	–	–	–	–	–	85.4	89.2	86.1	83.6	83.9
	WT	97.4	95.6	96.1	97.5	94.7	98.3	98.6	96.3	97.8	95.6	98.5	97.9
	UGS	79.3	78.5	80.1	81.2	77.2	78.6	77.9	–	–	–	–	–
	CEM	94.1	87.2	87.9	84.2	93.3	88.8	91.2	91.9	90.3	86.8	94.4	–
	BS	–	–	–	–	–	89.1	–	–	–	–	–	–
	OA (%)	86.2	82.8	82.9	84.7	84.1	85.1	85.1	85.3	86.5	83.9	86.1	84.7
	Kappa	0.84	0.79	0.80	0.82	0.82	0.83	0.83	0.83	0.84	0.81	0.84	0.83
2016													
Aggregated class accuracy	HDB	87.7	–	–	88.9	85.4	89.6	–	–	–	–	–	–
	LDB	75.4	71.3	72.6	70.5	71.2	68.4	69.2	66.4	65.8	72.2	71.9	71.5
	AGR	92.5	82.6	85.7	87.3	85.5	87.7	90.3	90.9	89.5	86.6	88.7	89.4
	FR	–	–	–	–	–	–	–	89.9	91.4	86.9	87.8	88.9
	WT	98.9	94.9	96.8	97.6	95.2	96.5	98.8	96.9	97.8	97.1	99.1	98.4
	UGS	81.6	79.7	81.1	83.7	79.9	81.6	81.4	–	–	–	–	–
	CEM	94.6	88.8	91.7	86.8	93.2	91.6	93.5	94.2	91.7	89.8	94.6	–
	BS	–	–	–	–	–	90.4	–	–	–	–	–	–
	OA (%)	88.4	83.5	85.6	85.5	85.1	86.5	86.6	87.6	87.2	86.5	88.4	87.1
	Kappa	0.86	0.81	0.83	0.83	0.83	0.85	0.85	0.86	0.85	0.85	0.86	0.85

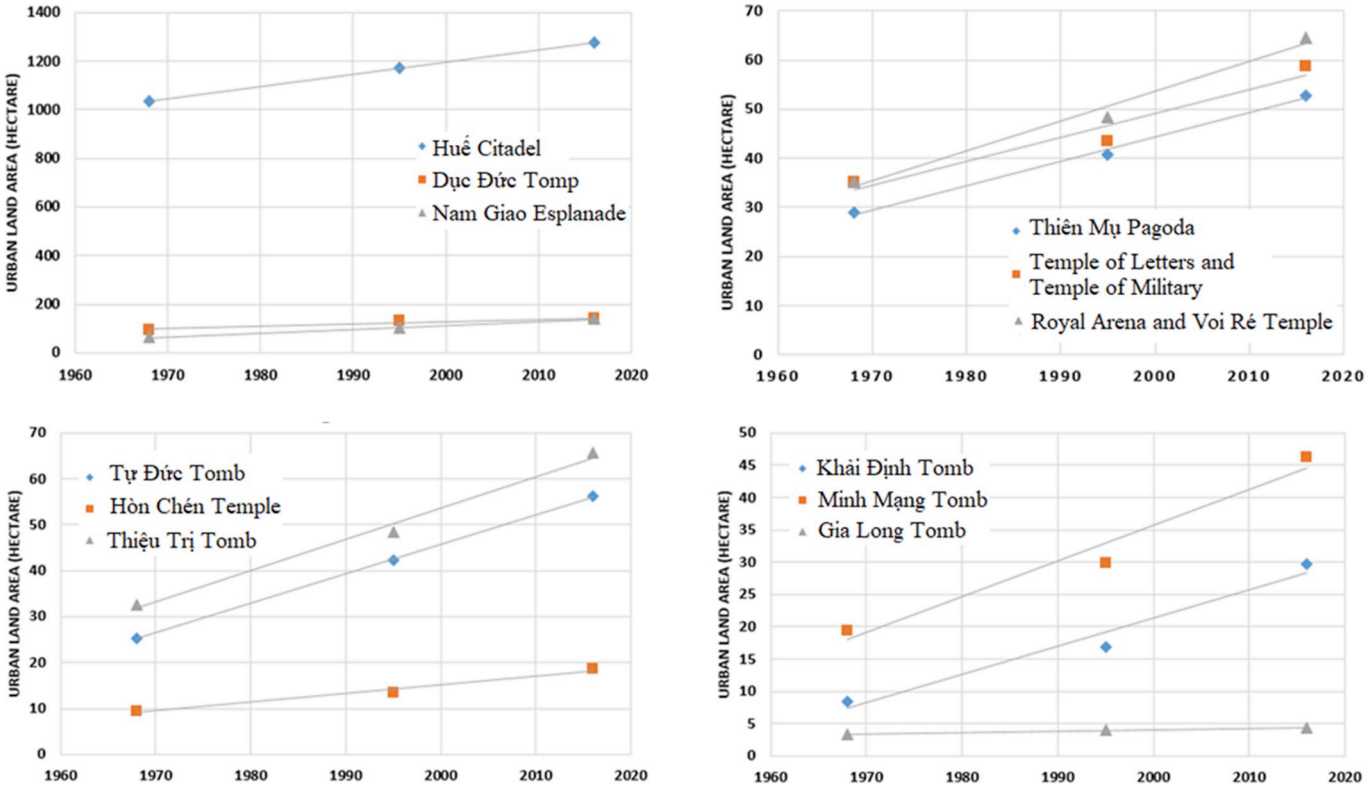

Fig. 6. Scatter plots of urban land areas for 12 sites in the period of 1968–2016.

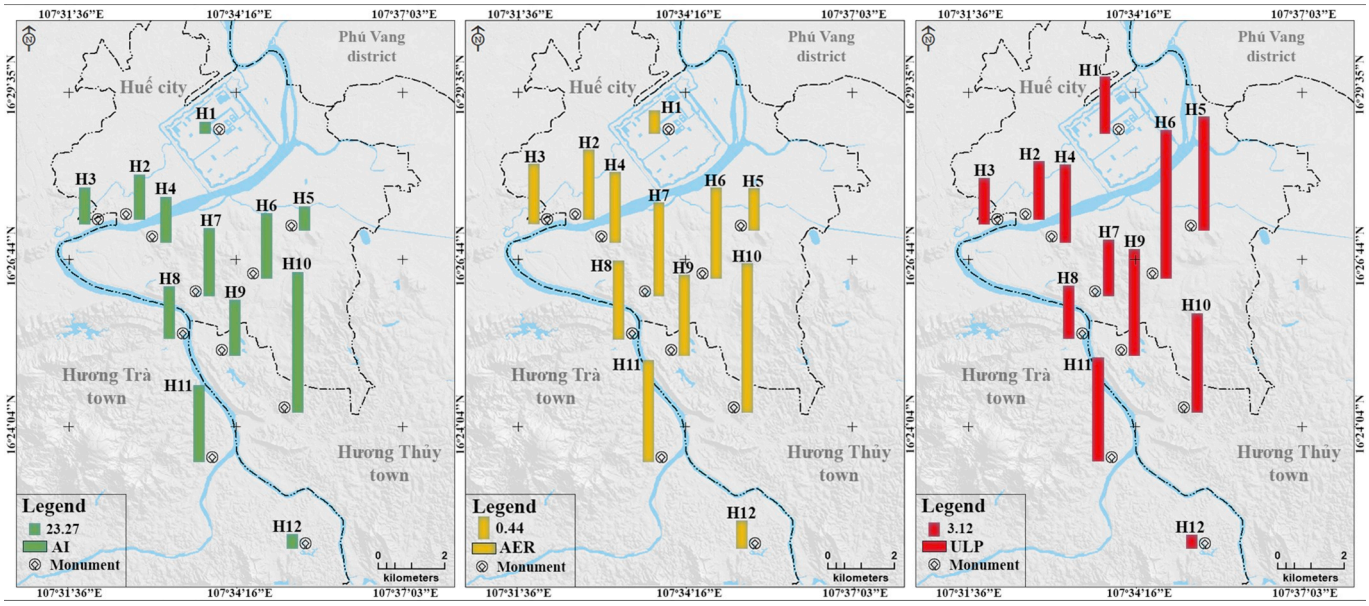

Fig. 7. Annual Increase (AI) in the left panel, Annual Expansion Rate (AER) in the center panel, and Urban Land Percentage (ULP) in the right panel in the period of 1968–2016 for the 12 sites: Huế Citadel (H1), Thiên Mụ Pagoda (H2), Temple of Letters and Temple of Military (H3), Royal Arena and Voi Ré Temple (H4), Dục Đức Tomb (H5), Nam Giao Esplanade (H6), Tự Đức Tomb (H7), Hòn Chén Temple (H8), Thiệu Trị Tomb (H9), Khải Định Tomb (H10), Minh Mạng Tomb (H11), and Gia Long Tomb (H12).

Table 4
Urban Green Infrastructure (UGI) in seven sites: Huế Citadel (H1), Thiên Mụ Pagoda (H2), Temple of Letters and Temple of Military (H3), Royal Arena and Voi Ré Temple (H4), Dục Đức Tomb (H5), Nam Giao Esplanade (H6), Tự Đức Tomb (H7).

1968	Area (ha)	1995	Area (ha)	2016	Area (ha)	% (1968–1995)	% (1995–2016)	% (1968–2016)
H1	232.59	H1	171.62	H1	175.99	−26.21	2.55	−24.33
H2	39.86	H2	43.23	H2	41.90	8.45	−3.08	5.12
H3	67.11	H3	63.83	H3	60.68	−4.89	−4.93	−9.58
H4	63.17	H4	60.53	H4	57.63	−4.18	−4.79	−8.77
H5	39.73	H5	19.39	H5	14.60	−51.20	−24.70	−63.25
H6	69.96	H6	69.17	H6	57.04	−1.13	−17.54	−18.47
H7	169.07	H7	153.03	H7	148.91	−9.49	−2.69	−11.92

than between 1968 and 1995. A modest increase of urban areas can be observed over 48 years in the 12 sites, corresponding to an expansion of about 39% of their original extent.

Good UGS at some monument sites (Fig. 5 and Table 4), such as Tự Đức Tomb, is attributable to the landscape improvement of the monuments that have become more blended to natural surroundings. It should be noted that the Nguyễn Dynasty developed the Huế Citadel and the monuments in consideration of trees and green spaces to embellish the structures, making the massive built-up structures become harmonious with nature, rivers, streams, and the overall landscape. In contrast, contemporary haphazard urbanization has inflicted imbalance and negative impacts on the sustainable development of Huế City.

3.3. Evaluation of the impacts in the perspective of quantifying ecosystem services

This research attempts to evaluate and quantify urbanization patterns and resulting impacts on the natural environment around the monuments. The sums of all ecosystem services (ES) values from the period 1968 to 2016 of 12 monuments and for each contributing class are summarized in Table 5. A total absolute loss (TAL) in ES values can be observed among all LCLU classes except bare soil (BS) and cemetery (CEM). Over the 48-year period, the increase of high-density built-up (HDB) and low-density built-up (LDB) areas occurred at the cost of other LCLU classes, predominately through the transition from agricultural land and vegetation cover into urban and built-up areas. During the same period, greenery (UGS) that had formerly existed along the main roads around the monuments was transformed to LDB and HDB.

The loss of ES values is primarily contributed by agriculture (AGR), greenery (UGS), and forest (FR), followed by water bodies such as lakes and rivers (WT) because these four classes account for the most ecosystem functions. Substantial losses in AGR and UGS can be observed in Voi Ré Temple, Dục Đức Tomb, and Nam Giao Esplanade, with AGR reductions of 55%, 75%, and 74%, and with UGS losses of about 9%, 63%, and 18%, respectively, whereas the urban indicators show an increase (Fig. 6). Similar results are also observed in Thiên Mụ Pagoda, and Temple of Letters and Temple of Military. These results signify a negative impact because the monuments have suffered adverse effects from the process of haphazard urbanization. HDB areas have appeared in more monument sites, while LDB has developed with additional construction in existing urban areas. HDB areas often have significant negative impacts around these monuments because of industrial and commercial activities and high population density with small or no green space. Because of the presence of some vegetation cover and less intense socioeconomic factors, LDB areas have less significant negative impacts on monuments than do HDB areas. Table 5 reveals especially strong impacts with TAL = −0.24 at Huế Citadel and TAL = −0.20 at Nam Giao Esplanade. The main reason for this loss is the reduction of AGR and UGS for the increase in HDB at Huế Citadel, and in both HDB and LDB at Nam Giao Esplanade. The overall sum of TAL = −0.44 million US dollars is found for all 12 sites in the period from 1968 to 2016. The increase in HDB and LDB contribute to the reduction of the

Table 5
Ecosystem services value of each class, quantified in million US dollars applied for the period 1968–2016 for the 12 monuments: Huế Citadel (H1), Thiên Mụ Pagoda (H2), Temple of Letters and Temple of Military (H3), Royal Arena and Voi Ré Temple (H4), Dục Đức Tomb (H5), Nam Giao Esplanade (H6), Tự Đức Tomb (H7), Hòn Chén Temple (H8), Thiệu Trị Tomb (H9), Khải Định Tomb (H10), Minh Mạng Tomb (H11), and Gia Long Tomb (H12).

	LCLU Class	Year			TAL	Rate (%)		LCLU Class	Year			TAL	Rate (%)
		1968	1995	2016					1968	1995	2016		
H1	HDB	3.37	4.62	6.06	−2.69	+79.82	**H7**	LDB	0.17	0.28	0.37	−0.2	+117.64
	LDB	3.52	3.18	2.43	1.09	−30.96		WT	0.17	0.18	0.18	−0.01	+5.88
	WT	4.47	4.48	4.57	−0.1	+2.23		UGS	1.26	1.14	1.11	0.15	−11.09
	UGS	1.73	1.28	1.31	0.42	−24.28		AGR	0.26	0.22	0.15	0.11	−42.30
	AGR	1.62	1.18	0.58	1.04	−64.19			∑			***0.05***	
		∑			***−0.24***								
H2	LDB	0.19	0.27	0.35	−0.16	+84.21	**H8**	LDB	0.06	0.09	0.12	−0.06	+100
	WT	0.42	0.42	0.42	0	0		WT	0.38	0.39	0.38	0	0
	UGS	0.30	0.32	0.31	−0.01	+3.33		AGR	0.18	0.18	0.17	0.01	−5.55
	AGR	0.42	0.27	0.20	0.22	−52.38		FR	0.52	0.49	0.48	0.04	−7.69
		∑			***0.05***				∑			***−0.01***	
H3	LDB	0.23	0.29	0.39	−0.16	+69.56	**H9**	LDB	0.22	0.32	0.43	−0.21	+95.45
	WT	0.50	0.52	0.52	−0.02	+4		WT	0.46	0.46	0.45	0.01	−2.17
	UGS	0.50	0.48	0.45	0.05	−10		AGR	0.30	0.25	0.21	0.09	−30
	AGR	0.40	0.30	0.22	0.18	−45		FR	1.20	1.15	1.08	0.12	−10
		∑			***0.05***				∑			***0.01***	
H4	HDB	0.02	0.04	0.10	−0.08	+400	**H10**	LDB	0.05	0.11	0.19	−0.14	+280
	LDB	0.22	0.28	0.33	−0.11	+50		WT	0.05	0.04	0.03	0.02	−40
	WT	0.34	0.35	0.34	0	0		AGR	0.30	0.34	0.36	−0.06	+20
	UGS	0.47	0.45	0.43	0.04	−8.51		FR	1.62	1.54	1.43	0.19	−11.72
	AGR	0.20	0.16	0.09	0.11	−55			∑			***0.01***	
		∑			***−0.04***								
H5	HDB	0.18	0.57	0.78	−0.6	+333.33	**H11**	LDB	0.13	0.20	0.31	−0.18	+138.46
	LDB	0.46	0.30	0.14	0.32	−69.56		WT	0.52	0.52	0.56	−0.04	+7.69
	WT	0.06	0.06	0.06	0	0		AGR	0.19	0.17	0.16	0.03	−15.78
	UGS	0.30	0.14	0.11	0.19	−63.33		FR	1.62	1.58	1.48	0.14	−8.64
	AGR	0.04	0.03	0.01	0.03	−75			∑			***−0.05***	
		∑			***−0.06***								
H6	HDB	0.07	0.13	0.30	−0.23	+328.57	**H12**	LDB	0.02	0.03	0.03	−0.01	+50
	LDB	0.36	0.54	0.63	−0.27	+75		WT	0.09	0.09	0.09	0	0
	WT	0.01	0.00	0.00	0.01	−100		AGR	0.06	0.10	0.10	−0.04	+66.66
	UGS	0.52	0.52	0.43	0.09	−17.31		FR	0.57	0.53	0.53	0.04	−7.01
	AGR	0.27	0.15	0.07	0.2	−74.07			∑			***−0.01***	
		∑			***−0.20***								

overall TAL with a total growth of about 559 ha in urban areas, while the loss of both AGR and UGS together accounts for about 60% of the total loss of ES values.

In general, urbanization impacts on the monuments vary considerably among the different locations as seen in Table 5, indicating the large heterogeneity in the spatial patterns of effects on different monument areas. Most of the green spaces (including greenery, agriculture, and forest) have decreased during the entire period. Such decrease possibly caused ecological imbalances in the process of urban development, leading to a degradation of the landscape of the monument areas. The ecosystem services analysis has provided consistent results for the Complex of Huế Monuments, where urban expansion and landscape changes have had significant detrimental effects on the monuments. However, current evaluation approaches are not sufficiently refined to capture smaller and yet important losses in ecosystem services functions and their values for these monuments. Relative changes in different land cover and land use classes at different monument areas enable an assessment of the spatial heterogeneity around each historical monument site. Nonetheless, assigning ecosystem services values to urban land cover and land use classes in the monument areas can be further complicated by the complex functions of the monuments and interactions with human socioeconomic activities and drivers from different management priorities and policy changes. In consideration of these complexities, ecosystem services might suffice as a relevant comparative indicator, but ecosystem services alone might not account for a complete evaluation of urbanization effects on the 12 monuments.

Due to the urbanization and the expansion of urban land area, the Complex of Huế Monuments has changed dramatically. Such significant change has evoked the process of land-use conversion, leading to contradictive decisions in urban development planning (HMCC, 2015), which have greatly affected the cultural heritage. The monuments have been under a huge pressure from settlements and living of citizens in the surrounding zone and from developments of the road infrastructure and modern constructions in and around the Complex of Huế Monuments as well as the increasing demand to support the rapid expansion of tourism in Thừa Thiên-Huế province (TTHPPC, 2013). Among the consequences is an irregular decline in agricultural land and greenery, which leads to a remarkable heterogeneity in the features of the landscape in space and in time. In addition, the encroachment of the relic buffer zone in the process of urbanization can contribute to the degradation of these heritages. For instance, the expansion of modern transportation infrastructure (such as new highways, etc.) damaged the Chóp Vung and Ngọc Trẩn mountain in front of the Tombs made "Tả Thanh Long", which is culturally considered as a feng-shui element of Khải Định and Minh Mạng Tombs. The endless traffic noise and visual pollution has deteriorated the veneration and the peacefulness of the complex of Huế monuments. In the construction of high-rise commercial centers in the Huế Citadel area, the parking area at Tự Đức Tomb has broken the coherent connectivity of the landscapes. Future land use plan must consider the precious value of these monuments to maintain their historical significance recognized as a UNESCO World Cultural Heritage.

4. Conclusions

This paper has presented an integrated approach to analyzing effects of land-use on historic monuments based on a combination of ecosystem services values and land cover and land use classifications to quantify urbanization effects on the Complex of Huế Monuments. With the

successful use of Support Vector Machine classifiers, remote-sensing data at high resolutions have been proven effective in monitoring urbanization trends at multiple scales in time and in space, while the synthesis interpretation has provided insights into impacts of urbanization.

The results of this study reveal valuable information about urbanization rates, trends, intensity, and patterns, and their impacts on 12 sites in the Complex of Huế Monuments. In the study region, a 559-ha increase in urban areas was detected. This urban increase in both high-density built-up (HDB) and low-density built-up (LDB) areas was predominately due to agriculture (AGR) and greenery (UGS) areas. An urban green index (UGI), a ratio of UGS to HDB/LDB areas, was calculated to relate the decrease in UGS to the corresponding growth in urban areas. The integrated approach demonstrated in this study to quantify urbanization impacts on the Huế historical monuments can be adapted to analyze effects of urbanization on other heritage sites across the world.

This study highlights the need for a sustainable urban development in these historic regions to mitigate adverse effects on the monuments and their surrounding environments. The integration of urbanization indices and ecosystem services is found effective for relative comparisons and for quantifying land cover and land use changes among different regions. High accuracies of change detection were achieved for three changing periods in terms of the overall accuracy (OA) and Kappa coefficient indexes. The results showed that the proposed method using high-resolution satellite data together with archived survey maps outperformed conventional post-classification in terms of assessment indexes. Nevertheless, limitations remain with manual spatial postprocessing steps that need to be automated.

Efficient methods using satellite remote sensing data with finer spatial resolutions are still a promising and attractive direction to assess rates of land cover and land use transformations, and to obtain values of ecosystem services in relations with human impacts. Thus, a complete evaluation of the explicit implications of urbanization will require both theoretical foundation and practical knowledge of the intricate interactions between natural and human processes and between cultural heritage and ecosystem services in future research. Such knowledge will be imperative for decision makers from responsible agencies to develop and implement effective policies for the preservation of the Complex of Huế Monuments in particular and other historical sites in general.

Acknowledgments

The research performed at the Vietnam National University, Hanoi University of Science, was supported by the Space Science and Technology Program, Vietnam Academy of Science and Technology (VAST). The research carried out at the Jet Propulsion Laboratory (JPL), California Institute of Technology, was supported by the National Aeronautics and Space Administration (NASA) Land-Cover and Land-Use Change (LCLUC) Program. We appreciate the coordination of the U.S. Department of State and the U.S. Embassy together with the Rector's Office of the Vietnam National University (VNU) Hanoi University of Science (HUS) for the science team meeting in Hanoi leading to this research collaboration between VNU HUS and NASA JPL. We thank Dr. Claire Marie-Peterson, a JPL senior technical editor and a native speaker of English, for proofreading the manuscript. Additional review and edits from Mr. Gregory Neumann, a senior staff at JPL and a native speaker of English, are also acknowledged.

Appendix A. Supplementary data

Supplementary data to this article can be found online at https://doi.org/10.1016/j.apgeog.2019.102096.

References

Alamgir, M., Pert, P. L., & Turton, S. M. (2014). A review of ecosystem services research in Australia reveals a gap in integrating climate change and impacts on ecosystem services. *International Journal of Biodiversity Science, Ecosystem Services & Management, 10*, 112–127. https://doi.org/10.1080/21513732.2014.919961.

Aldwaik, S. Z., & Pontius, R. G. (2012). Intensity analysis to unify measurements of size and stationarity of land changes by interval, category, and transition. *Landscape and Urban Planning, 106*, 103–114. https://doi.org/10.1016/j.landurbplan.2012.02.010.

Ban, Y., & Jacob, A. (2013). Object-based fusion of multitemporal multiangle ENVISAT ASAR and HJ-1B multispectral data for urban land-cover mapping. *IEEE Transactions on Geoscience and Remote Sensing, 51*, 1998–2006. https://doi.org/10.1109/TGRS.2012.2236560.

Ban, Y., Jacob, A., & Gamba, P. (2015). Spaceborne SAR data for global urban mapping at 30m resolution using a robust urban extractor. *ISPRS Journal of Photogrammetry and Remote Sensing, 103*, 28–37. https://doi.org/10.1016/j.isprsjprs.2014.08.004.

Bhaskaran, S., Paramananda, S., & Ramnarayan, M. (2010). Per-pixel and object-oriented classification methods for mapping urban features using Ikonos satellite data. *Applied Geography, 30*, 650–665. https://doi.org/10.1016/j.apgeog.2010.01.009.

Blaschke, T. (2010). Object-based image analysis for remote sensing. *ISPRS Journal of Photogrammetry and Remote Sensing, 65*, 2–16. https://doi.org/10.1016/j.isprsjprs.2009.06.004.

Bolund, P., & Hunhammar, S. (1999). Ecosystem services in urban areas. *Ecological Economy, 29*, 293–301. https://doi.org/10.1016/S0921-8009(99)00013-0.

Chavez, J., & Pat. (1996). *Image-based atmospheric corrections - revisited and improved*.

Chen, M., Liu, W., & Lu, D. (2016). Challenges and the way forward in China's new-type urbanization. *Land Use Policy, 55*, 334–339. https://doi.org/10.1016/j.landusepol.2015.07.025.

Corbane, C., Lang, S., Pipkins, K., Alleaume, S., Deshayes, M., García Millán, V. E., et al. (2015). Remote sensing for mapping natural habitats and their conservation status – new opportunities and challenges. *International Journal of Applied Earth Observation and Geoinformation, 37*, 7–16. https://doi.org/10.1016/j.jag.2014.11.005.

Cortes, C., & Vapnik, V. (1995). Support-vector networks. *Machine Learning, 20*, 273–297. https://doi.org/10.1007/BF00994018.

Costanza, R., de Groot, R., Sutton, P., van der Ploeg, S., Anderson, S. J., Kubiszewski, I., et al. (2014). Changes in the global value of ecosystem services. *Global Environmental Change, 26*, 152–158. https://doi.org/10.1016/j.gloenvcha.2014.04.002.

Costanza, R., d'Arge, R., & de Groot, R. (1997). *The value of the world's ecosystem services and natural capital* (Vol. 387, pp. 253–260).

De Groot, R., Brander, L., van der Ploeg, S., Costanza, R., Bernard, F., Braat, L., et al. (2012). Global estimates of the value of ecosystems and their services in monetary units. *Ecosystem Services, 1*, 50–61. https://doi.org/10.1016/j.ecoser.2012.07.005.

De Pinho, C. M. D., Fonseca, L. M. G., Korting, T. S., de Almeida, C. M., & Kux, H. J. H. (2012). Land-cover classification of an intra-urban environment using high-resolution images and object-based image analysis. *International Journal of Remote Sensing, 33*, 5973–5995. https://doi.org/10.1080/01431161.2012.675451.

Deng, J. S., Wang, K., Hong, Y., & Qi, J. G. (2009). Spatio-temporal dynamics and evolution of land use change and landscape pattern in response to rapid urbanization. *Landscape and Urban Planning, 92*, 187–198. https://doi.org/10.1016/j.landurbplan.2009.05.001.

Department of Survey, Mapping and Geographic Information of Vietnam. (2017). *The collection of aerial photos in Huế city in the period of 1960-1975*. Vietnam: Ministry of Natural Resources and Environment.

Dewan, A. M., & Yamaguchi, Y. (2009). Land use and land cover change in Greater Dhaka, Bangladesh: Using remote sensing to promote sustainable urbanization. *Applied Geography, 29*, 390–401. https://doi.org/10.1016/j.apgeog.2008.12.005.

Duro, D. C., Franklin, S. E., & Dubé, M. G. (2012). A comparison of pixel-based and object-based image analysis with selected machine learning algorithms for the classification of agricultural landscapes using SPOT-5 HRG imagery. *Remote Sensing of Environment, 118*, 259–272. https://doi.org/10.1016/j.rse.2011.11.020.

Erener, A. (2013). Classification method, spectral diversity, band combination and accuracy assessment evaluation for urban feature detection. *International Journal of Applied Earth Observation and Geoinformation, 21*, 397–408. https://doi.org/10.1016/j.jag.2011.12.008.

Estoque, R. C., & Murayama, Y. (2015). Intensity and spatial pattern of urban land changes in the megacities of Southeast Asia. *Land Use Policy, 48*, 213–222. https://doi.org/10.1016/j.landusepol.2015.05.017.

Feng, X., Fu, B., Yang, X., & Lü, Y. (2010). Remote sensing of ecosystem services: An opportunity for spatially explicit assessment. *Chinese Geographical Science, 20*, 522–535. https://doi.org/10.1007/s11769-010-0428-y.

Furberg, D. (2014). *Satellite monitoring of urban growth and indicator-based assessment of environmental impact. Architecture and the Built Environment*. Stockholm: KTH Royal Institute of Technology.

Gao, B., Huang, Q., He, C., Sun, Z., & Zhang, D. (2016). How does sprawl differ across cities in China? A multi-scale investigation using nighttime light and census data. *Landscape and Urban Planning, 148*, 89–98. https://doi.org/10.1016/j.landurbplan.2015.12.006.

Gao, H., Tang, Y., Jing, L., Li, H., & Ding, H. (2017). A novel unsupervised segmentation quality evaluation method for remote sensing images. *Sensors, 17*, 2427. https://doi.org/10.3390/s17102427.

Gearey, B. R., Fletcher, W., & Fyfe, R. (2014). Managing, valuing, and protecting heritage resources in the twenty-first century: Peatland archaeology, the ecosystem services framework, and the kyoto protocol. *Conservation and Management of Archaeological Sites, 16*, 236–244. https://doi.org/10.1179/1350503315Z.00000000084.

Guo, Z., Zhang, L., & Li, Y. (2010). Increased dependence of humans on ecosystem services and biodiversity. *PLoS One, 5*, e13113. https://doi.org/10.1371/journal.pone.0013113.

Haas, J. (2016). *Remote sensing of urbanization and environmental impacts*. Stockholm: KTH Royal Institute of Technology.

Haas, J., & Ban, Y. (2014). Urban growth and environmental impacts in jing-jin-ji, the yangtze, river delta and the pearl river delta. *International Journal of Applied Earth Observation and Geoinformation, 30*, 42–55. https://doi.org/10.1016/j.jag.2013.12.012.

He, C., Liu, Z., Tian, J., & Ma, Q. (2014). Urban expansion dynamics and natural habitat loss in China: A multiscale landscape perspective. *Global Change Biology, 20*, 2886–2902. https://doi.org/10.1111/gcb.12553.

HMCC (Huế Monuments Conservation Centre). (2015). *Management plan of the complex of Huế monuments for the period 2015-2020, vision 203 269*.

Hølleland, H., Skrede, J., & Holmgaard, S. B. (2017). Cultural heritage and ecosystem services: A literature review. *Conservation and Management of Archaeological Sites, 19*, 210–237. https://doi.org/10.1080/13505033.2017.1342069.

Huang, X., Schneider, A., & Friedl, M. A. (2016). Mapping sub-pixel urban expansion in China using MODIS and DMSP/OLS nighttime lights. *Remote Sensing of Environment, 175*, 92–108. https://doi.org/10.1016/j.rse.2015.12.042.

ICOMOS. (1992). World heritage list, Huế. *678*, 124–128.

Kane, K., Connors, J. P., & Galletti, C. S. (2014). Beyond fragmentation at the fringe: A path-dependent, high-resolution analysis of urban land cover in phoenix, Arizona. *Applied Geography, 52*, 123–134. https://doi.org/10.1016/j.apgeog.2014.05.002.

Kantakumar, L. N., Kumar, S., & Schneider, K. (2016). Spatiotemporal urban expansion in Pune metropolis, India using remote sensing. *Habitat International, 51*, 11–22. https://doi.org/10.1016/j.habitatint.2015.10.007.

Kuang, W., Chi, W., Lu, D., & Dou, Y. (2014). A comparative analysis of megacity expansions in China and the U.S.: Patterns, rates and driving forces. *Landscape and Urban Planning, 132*, 121–135. https://doi.org/10.1016/j.landurbplan.2014.08.015.

Lakes, T., & Kim, H.-O. (2012). The urban environmental indicator "Biotope Area Ratio"—an enhanced approach to assess and manage the urban ecosystem services using high resolution remote sensing. *Ecological Indicators, 13*, 93–103. https://doi.org/10.1016/j.ecolind.2011.05.016.

Li, C., Li, J., & Wu, J. (2013). Quantifying the speed, growth modes, and landscape pattern changes of urbanization: A hierarchical patch dynamics approach. *Landscape Ecology, 28*, 1875–1888. https://doi.org/10.1007/s10980-013-9933-6.

Liu, Z., He, C., Zhang, Q., Huang, Q., & Yang, Y. (2012). Extracting the dynamics of urban expansion in China using DMSP-OLS nighttime light data from 1992 to 2008. *Landscape and Urban Planning, 106*, 62–72. https://doi.org/10.1016/j.landurbplan.2012.02.013.

Liu, T., & Yang, X. (2015). Monitoring land changes in an urban area using satellite imagery, GIS and landscape metrics. *Applied Geography, 56*, 42–54. https://doi.org/10.1016/j.apgeog.2014.10.002.

Luisetti, T., Jackson, E. L., & Turner, R. K. (2013). Valuing the European 'coastal blue carbon' storage benefit. *Marine Pollution Bulletin, 71*, 101–106. https://doi.org/10.1016/j.marpolbul.2013.03.029.

Maes, J., Barbosa, A., Baranzelli, C., Zulian, G., Batista e Silva, F., Vandecasteele, I., et al. (2015). More green infrastructure is required to maintain ecosystem services under current trends in land-use change in Europe. *Landscape Ecology, 30*, 517–534. https://doi.org/10.1007/s10980-014-0083-2.

Malinverni, E. S., Tassetti, A. N., Mancini, A., Zingaretti, P., Frontoni, E., & Bernardini, A. (2011). Hybrid object-based approach for land use/land cover mapping using high spatial resolution imagery. *International Journal of Geographical Information Science, 25*, 1025–1043. https://doi.org/10.1080/13658816.2011.566569.

Marull, J., Font, C., & Boix, R. (2015). Modelling urban networks at mega-regional scale: Are increasingly complex urban systems sustainable? *Land Use Policy, 43*, 15–27. https://doi.org/10.1016/j.landusepol.2014.10.014.

Melesse, A., Weng, Q., Thenkabail, P., & Senay, G. (2007). Remote sensing sensors and applications in environmental resources mapping and modelling. *Sensors, 7*, 3209–3241. https://doi.org/10.3390/s7123209.

Millennium Ecosystem Assessment (Program). (2005). In *Ecosystems and human well-being: Synthesis*. Washington, DC: Island Press.

Mörtberg, U., Haas, J., Zetterberg, A., Franklin, J. P., Jonsson, D., & Deal, B. (2013). Urban ecosystems and sustainable urban development—analysing and assessing interacting systems in the Stockholm region. *Urban Ecosystems, 16*, 763–782. https://doi.org/10.1007/s11252-012-0270-3.

Myint, S. W., Gober, P., Brazel, A., Grossman-Clarke, S., & Weng, Q. (2011). Per-pixel vs. object-based classification of urban land cover extraction using high spatial resolution imagery. *Remote Sensing of Environment, 115*, 1145–1161. https://doi.org/10.1016/j.rse.2010.12.017.

NIMA. (1968). *Topographic map of hue at scale of 1: 50,000, series L7014, national imagery and mapping agency*. Published by University of Texas Libraries. Download at: http://legacy.lib.utexas.edu/maps/topo/vietnam/txu-pclmaps-oclc-21713238-6541-4.jpg.

NIMA. (1968). *City map of hue at scale of 1: 12,500, edition 3-AMS (29 ETB), series L909, national imagery and mapping agency*. Published by University of Texas Libraries. Download at: http://legacy.lib.utexas.edu/maps/world_cities/txu-oclc-21740104-hue-1968.jpg.

Niu, X., & Ban, Y. (2013). Multi-temporal RADARSAT-2 polarimetric SAR data for urban land-cover classification using an object-based support vector machine and a rule-based approach. *International Journal of Remote Sensing, 34*, 1–26. https://doi.org/10.1080/01431161.2012.700133.

Palacios-Orueta, A., Huesca, M., Whiting, M. L., Litago, J., Khanna, S., Garcia, M., et al. (2012). Derivation of phenological metrics by function fitting to time-series of Spectral Shape Indexes AS1 and AS2: Mapping cotton phenological stages using MODIS time series. *Remote Sensing of Environment, 126*, 148–159. https://doi.org/10.1016/j.rse.2012.08.002.

Pontius, R. G., & Millones, M. (2011). Death to Kappa: Birth of quantity disagreement and allocation disagreement for accuracy assessment. *International Journal of Remote Sensing, 32*, 4407–4429. https://doi.org/10.1080/01431161.2011.552923.

Pu, R., Landry, S., & Yu, Q. (2011). Object-based urban detailed land cover classification with high spatial resolution IKONOS imagery. *International Journal of Remote Sensing, 32*, 3285–3308. https://doi.org/10.1080/01431161003745657.

Qian, Y., Zhou, W., Yan, J., Li, W., & Han, L. (2014). Comparing machine learning classifiers for object-based land cover classification using very high resolution imagery. *Remote Sensing, 7*, 153–168. https://doi.org/10.3390/rs70100153.

Schneiders, A., Van Daele, T., Van Landuyt, W., & Van Reeth, W. (2012). Biodiversity and ecosystem services: Complementary approaches for ecosystem management? *Ecological Indicators, 21*, 123–133. https://doi.org/10.1016/j.ecolind.2011.06.021.

Shackelford, A. K., & Davis, C. H. (2003). A combined fuzzy pixel-based and object-based approach for classification of high-resolution multispectral data over urban areas. *IEEE Transactions on Geoscience and Remote Sensing, 41*, 2354–2364. https://doi.org/10.1109/TGRS.2003.815972.

Singh, S. K., Srivastava, P. K., Szabó, S., Petropoulos, G. P., Gupta, M., & Islam, T. (2017). Landscape transform and spatial metrics for mapping spatiotemporal land cover dynamics using Earth Observation data-sets. *Geocarto International, 32*, 113–127. https://doi.org/10.1080/10106049.2015.1130084.

Small, C., & Elvidge, C. D. (2013). Night on Earth: Mapping decadal changes of anthropogenic night light in Asia. *International Journal of Applied Earth Observation and Geoinformation, 22*, 40–52. https://doi.org/10.1016/j.jag.2012.02.009.

Song, X.-P., Sexton, J. O., Huang, C., Channan, S., & Townshend, J. R. (2016). Characterizing the magnitude, timing and duration of urban growth from time series of Landsat-based estimates of impervious cover. *Remote Sensing of Environment, 175*, 1–13. https://doi.org/10.1016/j.rse.2015.12.027.

Su, S., Ma, X., & Xiao, R. (2014). Agricultural landscape pattern changes in response to urbanization at ecoregional scale. *Ecological Indicators, 40*, 10–18. https://doi.org/10.1016/j.ecolind.2013.12.013.

Syrbe, R.-U., & Walz, U. (2012). Spatial indicators for the assessment of ecosystem services: Providing, benefiting and connecting areas and landscape metrics. *Ecological Indicators, 21*, 80–88. https://doi.org/10.1016/j.ecolind.2012.02.013.

Tengberg, A., Fredholm, S., Eliasson, I., Knez, I., Saltzman, K., & Wetterberg, O. (2012). Cultural ecosystem services provided by landscapes: Assessment of heritage values and identity. *Ecosystem Services, 2*, 14–26. https://doi.org/10.1016/j.ecoser.2012.07.006.

Tianhong, L., Wenkai, L., & Zhenghan, Q. (2010). Variations in ecosystem service value in response to land use changes in Shenzhen. *Ecological Economy, 69*, 1427–1435. https://doi.org/10.1016/j.ecolecon.2008.05.018.

TTHPPC. (2013). *The modification of Huế city's master plan 2030 and vision 2050*. Thừa Thiên-Huế Provincial People's Committee (in Vietnamese).

UN-Habitat (Ed.). (2013). *Prosperity of cities, the state of the world's cities*. New York, NY: Routledge [u.a.].

Ustin, S. L., Darling, D., Kefauver, S., Greenberg, J., Cheng, Y.-B., & Whiting, M. L. (2004). *Remotely sensed estimates of crop water demand*. In W. Gao, & D. R. Shaw (Eds.) (p. 230).

Verbeek, T., Boussauw, K., & Pisman, A. (2014). Presence and trends of linear sprawl: Explaining ribbon development in the north of Belgium. *Landscape and Urban Planning, 128*, 48–59. https://doi.org/10.1016/j.landurbplan.2014.04.022.

Xie, G. D., Zhen, L., Lu, C. X., Xiao, Y., & Chen, C. (2008). *Expert knowledge based valuation method of ecosystem services in China*.

Yi, K., Zeng, Y., & Wu, B. (2016). Mapping and evaluation the process, pattern and potential of urban growth in China. *Applied Geography, 71*, 44–55. https://doi.org/10.1016/j.apgeog.2016.04.011.

Zhang, X., Feng, X., & Jiang, H. (2010). Object-oriented method for urban vegetation mapping using IKONOS imagery. *International Journal of Remote Sensing, 31*, 177–196. https://doi.org/10.1080/01431160902882603.

Zhang, Q., & Seto, K. C. (2011). Mapping urbanization dynamics at regional and global scales using multi-temporal DMSP/OLS nighttime light data. *Remote Sensing of Environment, 115*, 2320–2329. https://doi.org/10.1016/j.rse.2011.04.032.

Zhang, Q., & Su, S. (2016). Determinants of urban expansion and their relative importance: A comparative analysis of 30 major metropolitans in China. *Habitat International, 58*, 89–107. https://doi.org/10.1016/j.habitatint.2016.10.003.

Zhao, S., Zhou, D., Zhu, C., Qu, W., Zhao, J., Sun, Y., et al. (2015). Rates and patterns of urban expansion in China's 32 major cities over the past three decades. *Landscape Ecology, 30*, 1541–1559. https://doi.org/10.1007/s10980-015-0211-7.

Zhou, W., Huang, G., Troy, A., & Cadenasso, M. L. (2009). Object-based land cover classification of shaded areas in high spatial resolution imagery of urban areas: A comparison study. *Remote Sensing of Environment, 113*, 1769–1777. https://doi.org/10.1016/j.rse.2009.04.007.

Zhou, W., Qian, Y., Li, X., Li, W., & Han, L. (2014). Relationships between land cover and the surface urban heat island: Seasonal variability and effects of spatial and thematic resolution of land cover data on predicting land surface temperatures. *Landscape Ecology, 29*, 153–167. https://doi.org/10.1007/s10980-013-9950-5.